ACS Macro Letters

Letter

pubs.acs.org/macroletters

Photodirected Formation and Control of Wrinkles on a Thiol−ene Elastomer

Stephen J. Ma,[†] Samantha J. Mannino,[†] Norman J. Wagner,[†,‡] and Christopher J. Kloxin*[,†,§]

Departments of [†]Chemical and Biomolecular Engineering and [§]Materials Science and Engineering and [‡]Center for Molecular and Engineering Thermodynamics, University of Delaware, Newark, Delaware 19716, United States

Supporting Information

ABSTRACT: Photopolymerization on a thiol−ene elastomer is a novel method to spatiotemporally control wrinkle formation gradients and complex patterns. Acrylate-rich elastomers, containing photoinitiator and photoabsorber, were strained and irradiated with UV light to generate wrinkles in as little as five seconds. The presence of the photoabsorber confines the UV light to a thin skin layer, facilitating wrinkle formation upon release of the strain. In conjunction with photomasks, wrinkles are confined and oriented with explicit boundaries defined by the irradiation pattern. Using a photoorthogonal photoiniator, we also demonstrate the ability to independently control the bulk modulus of the wrinkled elastomer. The wide array of thiol and ene monomers, photoinitiators, and photomask designs result in an alternative approach that is rapid, facile, and highly versatile, further enabling the *a priori* design and engineering of surface topography and shape of the material.

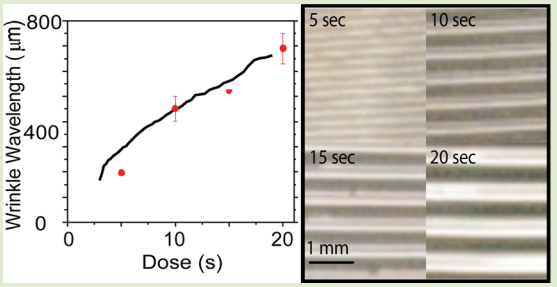

Recently, researchers have demonstrated the critical role surface topography plays on material interaction with the environment.[1−3] In nature, surface topography is responsible for a range of phenomena including the adhesion of gecko feet due to multiple length scales of nanohairs[4,5] and the superhydrophobicity of the lotus leaf.[6] Buckling or wrinkling of a polymer surface is a simple and versatile method for generating topologically structured surfaces with a large range of length-scales, which are controlled in part through the elasticity of the material. Such "wrinkled" surfaces have numerous applications such as antifouling coatings,[1,2,7] adhesives,[3] and microarray lenses with tunable focal lengths.[8]

Current strategies for creating surface topography on an elastomer via the wrinkling phenomenon utilize a two-step process: (1) deformation of the elastomeric foundation followed by (2) the application of a thin, high modulus skin layer that is physically or chemically bonded to the foundation. When the deformation of the foundation is released, the foundation exerts a lateral compressive force on the skin layer, generating wrinkles.[9−12] The wrinkling process itself is a consequence of a mechanical instability, where the initial geometry and elasticities as well as the boundary conditions are critical for engineering the surface topography.

The majority of the investigations of wrinkling phenomenon in elastomer materials utilize poly(dimethylsiloxane) PDMS because the surface is readily converted into a high modulus, thin silicate skin layer upon exposure to UV−ozone (UVO). A variety of techniques have been reported for deforming the PDMS foundation, including thermal expansion,[13,14] swelling,[15−17] and mechanical strain.[2,9,10,12,18−22] Bowden and coworkers demonstrated wrinkling through thermal expansion of a PDMS substrate followed by subsequent UVO treatment[13] or gold deposition[23] atop the heated surface. Upon cooling, the PDMS foundation will contract to its original size and the mismatch between the skin and foundation layers generates buckles. Crosby and co-workers presented a novel one-step swelling approach to wrinkle formation by using acrylic monomers to both form and swell the foundation layer using UV-oxygen.[15] Lin et al.[12] established the ability to create well-ordered herringbone structures through sequential biaxial mechanical strain on PDMS.

Despite this growing body of research, the precise control and orientation of the wrinkle formation necessary to engineer the surface topography for specific applications remains a challenge. Spatial variations of modulus can direct wrinkling through lateral stress-dissipation, which results in the alignment of wrinkles perpendicular to regions of lower modulus.[10,13] However, as UVO treatment is a flood cure process, the spatial control of stress-dissipation has primarily been limited to physical stencils[10,13] or holes placed into the PDMS foundation[21] prior to UVO treatment. After UVO treatment, the unoxidized regions allow the harder silicate layer to dissipate the high lateral stress and direct wrinkling. Huck et al.[11] demonstrated a novel alternative to generate wrinkles, where PDMS was swollen in a dichloromethane-benzophenone solution and irradiated using photomasked UV light (254 nm, 10−30 min), resulting in a higher cross-link density in the exposed regions. The sample was subsequently heated, causing different extents of thermal expansion in the elastomer due to

Received: April 5, 2013
Accepted: May 9, 2013
Published: May 14, 2013

 © 2013 American Chemical Society

differences in the moduli between the exposed and the unexposed regions. These samples were also coated with gold prior to cooling, providing a greater modulus mismatch and enhancing wrinkling. Importantly, the photopatterned regions were shown to establish a boundary condition that directs the wrinkling phenomenon in a manner similar to the utilization of physical constraints.[11]

Nair et al.[24] recently demonstrated the utility of a two-stage polymerization approach in a range of material applications, from shape memory to index structures. Here, we employ a similar two-stage polymerization strategy where an elastomer is formed via one polymerization mechanism, but the second photopolymerization, which increases cross-link density, is restricted to the elastomer's surface. Specifically, a base elastomer is synthesized using a stoichiometric imbalance of tetra-thiol and diacrylate monomers, yielding a polymer network with excess acrylate functional groups (see Figure 1). Note that the initial thiol−ene polymerization is not inhibited by oxygen and cure times are significantly shorter than that of, for example, PDMS (~5 min, see Supporting Information, S1).[25] The second-stage, photopolymerization of the pendent acrylates is confined to a thin "skin" layer by introducing a photoabsorber (T328) into the formulation (see Supporting Information). Combining this approach with mechanical deformation (i.e., mechanophotopatterning)[26] enables wrinkle formation and confinement through photopatterning, rather than through physical defects or stencils, to design intricate patterns and facilitates control over wrinkle wavelength locally.

To generate wrinkles, the elastomer is mechanically stretched using linear stages. A skin layer is formed via photoinitiated radical homopolymerization of the pendant acrylate groups in the thiol−ene network in as little as 5 s, even in the presence of oxygen. As the second polymerization occurs within a very thin layer at the substrate surface, both irradiation time and oxygen exposure can be used to control the modulus and thickness of the skin layer. Oxygen can readily and continually diffuse into the matrix and will inhibit the acrylate polymerization. To further interrogate the effects of oxygen inhibition, samples with and without an oxygen barrier (i.e., coverslip) were examined with stylus profilometry. As shown in Figure 2a, samples employing a coverslip have significantly increased wrinkling wavelength owing to a higher modulus in the skin layer. As the irradiation dosage is increased, the wrinkle

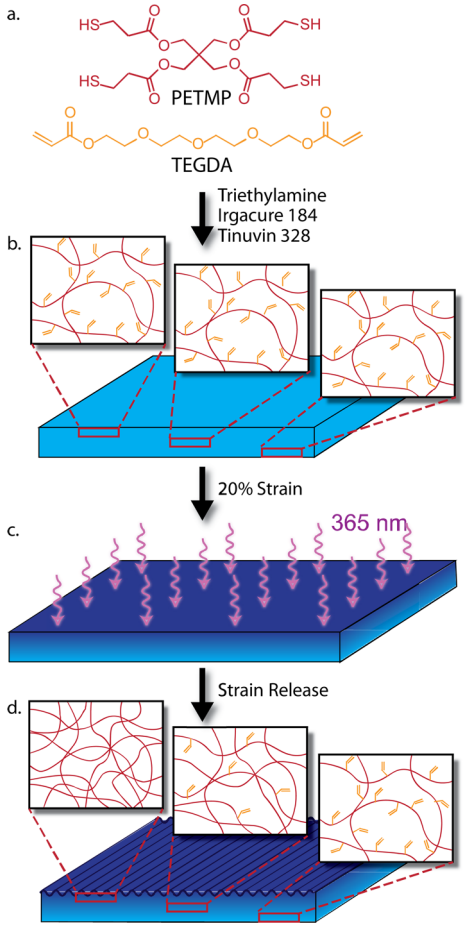

Figure 1. Method of Generating Wrinkles on a thiol−ene surface. Monomers (a) pentaerythritol tetramercaptopropionate (PETMP) and tetraethylene glycol diacrylate (TEGDA) were reacted with triethylamine, photoinitiator (I184), and photoabsorber (T328) to produce a (b) thiol−ene network with a uniform cross-link density and excess pendant acrylates (first-stage polymerization). (c) Applying strain and 365 nm light induces radical polymerization of the acrylates (second stage polymerization). The photoabsorber confines the light to a thin skin layer at the surface. (d) Upon releasing the strain on the film, wrinkles are formed with a cross-link density (modulus) gradient.

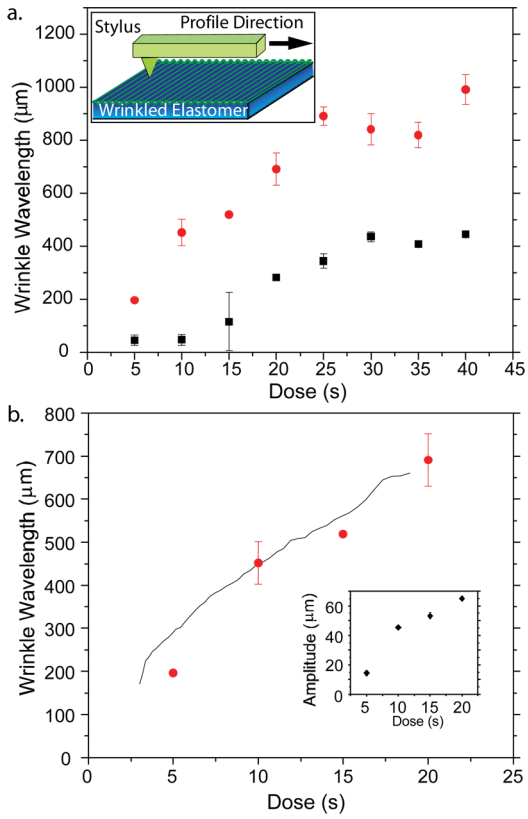

Figure 2. Stylus profilometry of wrinkle wavelength versus dosage. (a) Films with a coverslip (red circles) and without a coverslip oxygen barrier (black squares) were irradiated for 5−40 s using 365 nm light at 80 W/m^2. Wrinkle wavelength increased as a function of increasing dosage. Samples masked with a coverslip exhibited larger wrinkles than the unmasked samples due to the absence of oxygen inhibition. Inset: Stylus profilometry schematic. (b) Profilometry from wrinkle gradients (solid black line) shows good agreement with discrete wavelength data (red circles; 0−20 s, 365 nm at 80 W/m^2 with coverslip). Accompanying amplitude data (inset) are consistent with scaling equation (see Supporting Information for profilometry setup).

dx.doi.org/10.1021/mz400166e | ACS Macro Lett. 2013, 2, 474−477

wavelength increases with both the skin thickness and modulus (i.e., $\lambda_c \sim h(E_s/E_f)^{1/3}$, where λ_c is the wrinkle wavelength, h is the height of the skin layer, and E is elastic moduli and subscripts s and f denote the skin and foundation, respectively).[9,10]

It should be noted that our system does not have a well-defined foundation-skin interface, but rather a gradient in properties due to the attenuation of light with increasing depth into the elastomer. Using tapping mode AFM, we are able approximate E_s and E_f and, thus, calculate an "effective" skin thickness of 80 μm at 20 s UV exposure (see Supporting Information, Figures S4 and S5). As expected, this thickness is a function of irradiation dose. In the absence of inhibition, the polymerization rate is highest at the surface but decreases exponentially according to the Beer–Lambert law (i.e., $R_p \sim I^{1/2} \sim I_0 e^{-A/2}$, where I_0 is the incident intensity and A is absorption).[27] At longer cure times, the acrylates at the surface reach maximum conversion while the acrylates within the elastomer continue to photopolymerize. In this manner, a controlled frontal polymerization proceeds into the elastomer. The "effective" skin thickness is limited by the penetration depth of the light, which is dictated by the incident intensity and concentration of photoabsorber (i.e., T328). As a consequence, the wrinkle wavelength, shown in Figure 2a, increases with increasing dosage, but eventually plateaus for longer dose times. In contrast to the samples with coverslips, which show an immediate increase in wrinkle wavelength with dosage time, samples without coverslips show no significant change for the first 10 s, which we attribute to oxygen inhibition at the interface.[28]

Our approach of using photopolymerization to form wrinkles enables spatioselective control of the wrinkle wavelength. As a demonstration, we have created a wrinkled surface with a linear gradient wrinkle wavelength (Figure 2b). After the first-stage polymerization, samples with a coverslip oxygen barrier were strained and covered with an opaque photomask that was subsequently removed at a constant rate during irradiation over a 20 s period (via syringe pump setup, see Supporting Information, Figure S2). Profilometry data of the gradient wrinkles plotted in Figure 2b (solid black line) shows the local wrinkle topology is in good agreement with experiments performed at the corresponding, uniform irradiation doses (red circles). These gradient wrinkles will facilitate experiments to probe surface interactions over a continuum of length scales on the same sample. Wrinkle amplitudes (Figure 2b (inset)) are on the micrometer scale and increase with increasing dosage.

Our method also presents a novel approach to direct wrinkling using a photomask (Figure 3a). The regions of the polymer substrate that are exposed to light undergo the second-stage polymerization, while the masked areas remain unchanged, thereby creating well-defined boundaries for wrinkle confinement. The low modulus regions allow the high modulus regions to relieve in-plane stresses, aligning the wrinkles perpendicular to the boundary of the mask. This is particularly advantageous because no additional chemical treatments are required nor are extra physical defects introduced into the polymer foundation. This approach provides a rapid method for generating wrinkles on an untreated thiol–ene foundation with excellent pattern fidelity. Moreover, by overlaying photomasks and irradiating the substrates in a stepwise manner, we can form several distinct wavelengths. This sequential masking introduces a pattern with controlled variations in irradiation on the elastomer, resulting in

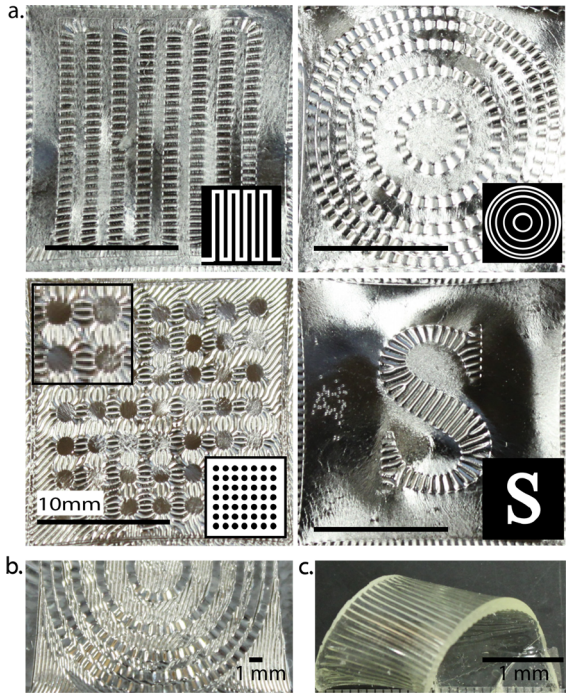

Figure 3. Wrinkle formation via photopatterning on a biaxially stretched specimen. (a) Photolithography guides the alignment of the wrinkles perpendicular to the low stress regions of the thiol–ene elastomer. Samples were irradiated for 20 s under 365 nm light at 80 W/m^2. Scale bar represents 10 mm (inset: corresponding photomasks). (b) Photopolymerized sample showing alternating wrinkle wavelengths. This pattern is created by stepwise dosing, first with a coverslip only (80 W/m^2, 5 s) followed by two photomasks (80 W/m^2, 5 s, and 80 W/m^2, 10 s). (c) Employing two different photoinitiators allows for wrinkle formation and shape memory. Wrinkles were formed using a procedure similar to (a). The coil shape was held in place using tape and exposed to 405 nm light (60 W/m^2, 16 min).

the novel wrinkle patterns shown in Figure 3b. The longer wavelengths are a consequence of longer exposure times, while the second alternating pattern contains smaller wrinkles.

Last, we illustrate the ability to use two photo-orthogonal photoinitiators to independently control surface wrinkling and increase the *bulk* modulus of the material. As the photoabsorber, T328, is transparent above 400 nm, a second, visible light photoinitiator can be utilized to trigger polymerization of acrylates in the bulk. A visible light photoinitiator, I819, which absorbs above 400 nm, was added to the monomer formulation prior to the first-stage polymerization. Wrinkles were created using the aforementioned procedures with 365 nm light. The film was held in a coil shape and exposed to 405 nm light (Figure 3c). The resulting bulk polymerization creates new cross-links, significantly increasing the modulus and thus "locking" the shape while maintaining the wrinkled surface. Thus, the foundation and skin layer moduli can be controlled independently to affect the material shape and topography, respectively. This may have benefits for engineering surface-wrinkled materials with a broader range of surface and bulk moduli.

Photopolymerization is a novel approach to spatioselectively control wrinkle formation, including gradients and complex patterns. Our system is highly tunable; modifying the types and amounts of photoabsorber, photoinitiator, and thiol–ene monomers, as well as utilizing different light wavelengths and

dx.doi.org/10.1021/mz400166e | *ACS Macro Lett.* 2013, 2, 474–477

intensities provides multiple controls over the mechanical properties, shape, and surface topography of the material. Photo-orthogonality not only allows wrinkle formation, but also enables the bulk polymer to be molded into desired geometries. The implementation of surface confined polymerization in a thiol−ene elastomer presents an attractive alternative to PDMS and other elastomers for the exploration of wrinkling phenomenon and ultimately for the a priori design and engineering of surface topography.

■ ASSOCIATED CONTENT

Supporting Information

Experimental details, images of experimental setups, profilometry settings, and kinetic study of thiol−ene reaction. This material is available free of charge via the Internet at http://pubs.acs.org.

■ AUTHOR INFORMATION

Corresponding Author

*E-mail: cjk@udel.edu. Fax: +302 8311048. Tel.: +302 8318670.

Notes

The authors declare no competing financial interest.

■ ACKNOWLEDGMENTS

This research was supported by NSF Grant No. 1247394. The authors thank Dr. Jeffrey Meth and Steve Zane (DuPont) for their assistance with profilometry and for helpful discussions.

■ REFERENCES

(1) Schumacher, J. F.; Carman, M. L.; Estes, T. G.; Feinberg, A. W.; Wilson, L. H.; Callow, M. E.; Callow, J. A.; Finlay, J. A.; Brennan, A. B. *Biofouling* **2007**, *23*, 55−62.
(2) Efimenko, K.; Finlay, J.; Callow, M. E.; Callow, J. A.; Genzer, J. *ACS Appl. Mater. Interfaces* **2009**, *1*, 1031−1040.
(3) Davis, C. S.; Martina, D.; Creton, C.; Lindner, A.; Crosby, A. J. *Langmuir* **2012**, *28*, 14899−14908.
(4) Autumn, K.; Liang, Y. A.; Hsieh, S. T.; Zesch, W.; Chan, W. P.; Kenny, T. W.; Fearing, R.; Full, R. J. *Nature* **2000**, *405*, 681−685.
(5) Autumn, K.; Sitti, M.; Liang, Y. C. A.; Peattie, A. M.; Hansen, W. R.; Sponberg, S.; Kenny, T. W.; Fearing, R.; Israelachvili, J. N.; Full, R. J. *Proc. Natl. Acad. Sci. U.S.A.* **2002**, *99*, 12252−12256.
(6) Feng, L.; Li, S. H.; Li, Y. S.; Li, H. J.; Zhang, L. J.; Zhai, J.; Song, Y. L.; Liu, B. Q.; Jiang, L.; Zhu, D. B. *Adv. Mater.* **2002**, *14*, 1857−1860.
(7) Schumacher, J. F.; Aldred, N.; Callow, M. E.; Finlay, J. A.; Callow, J. A.; Clare, A. S.; Brennan, A. B. *Biofouling* **2007**, *23*, 307−317.
(8) Chandra, D.; Yang, S.; Lin, P.-C. *Appl. Phys. Lett.* **2007**, 91.
(9) Yang, S.; Khare, K.; Lin, P.-C. *Adv. Funct. Mater.* **2010**, *20*, 2550−2564.
(10) Genzer, J.; Groenewold, J. *Soft Matter* **2006**, *2*, 310−323.
(11) Huck, W. T. S.; Bowden, N.; Onck, P.; Pardoen, T.; Hutchinson, J. W.; Whitesides, G. M. *Langmuir* **2000**, *16*, 3497−3501.
(12) Lin, P. C.; Yang, S. *Appl. Phys. Lett.* **2007**, 90.
(13) Bowden, N.; Huck, W. T. S.; Paul, K. E.; Whitesides, G. M. *Appl. Phys. Lett.* **1999**, *75*, 2557−2559.
(14) Chan, E. P.; Lin, Q.; Stafford, C. M. *J. Polym. Sci., Part B: Polym. Phys.* **2012**, *50*, 1556−1561.
(15) Chandra, D.; Crosby, A. J. *Adv. Mater.* **2011**, *23*, 3441−3445.
(16) Kim, H. S.; Crosby, A. J. *Adv. Mater.* **2011**, *23*, 4188−4192.
(17) Breid, D.; Crosby, A. J. *Soft Matter* **2013**, *9*, 3624−3630.
(18) Efimenko, K.; Rackaitis, M.; Manias, E.; Vaziri, A.; Mahadevan, L.; Genzer, J. *Nat. Mater.* **2005**, *4*, 293−297.
(19) Lin, P.-C.; Vajpayee, S.; Jagota, A.; Hui, C.-Y.; Yang, S. *Soft Matter* **2008**, *4*, 1830−1835.
(20) Lin, P.-C.; Yang, S. *Soft Matter* **2009**, *5*, 1011−1018.
(21) Chua, D. B. H.; Ng, H. T.; Li, S. F. Y. *Appl. Phys. Lett.* **2000**, *76*, 721−723.
(22) Davis, C. S.; Crosby, A. J. *J. Polym. Sci., Part B: Polym. Phys.* **2012**, *50*, 1225−1232.
(23) Bowden, N.; Brittain, S.; Evans, A. G.; Hutchinson, J. W.; Whitesides, G. M. *Nature* **1998**, *393*, 146−149.
(24) Nair, D. P.; Cramer, N. B.; Gaipa, J. C.; McBride, M. K.; Matherly, E. M.; McLeod, R. R.; Shandas, R.; Bowman, C. N. *Adv. Funct. Mater.* **2012**, *22*, 1502−1510.
(25) Chan, J. W.; Hoyle, C. E.; Lowe, A. B.; Bowman, M. *Macromolecules* **2010**, *43*, 6381−6388.
(26) Kloxin, C. J.; Scott, T. F.; Park, H. Y.; Bowman, C. N. *Adv. Mater.* **2011**, *23*, 1977−1981.
(27) Odian, G. *Principles of Polymerization*, 4th ed.; John Wiley & Sons, Inc.: Hoboken, NJ, 2004.
(28) O'Brien, A. K.; Bowman, C. N. *Macromol. Theor. Simul.* **2006**, *15*, 176−182.